**Atmospheric
Chemistry
and Physics
Discussions**

ACPD

5, 455–480, 2005

**Decrease in the
tropical mean
outgoing shortwave
radiation**

N. Hatzianastassiou et al.

Analysis of the decrease in the tropical mean outgoing shortwave radiation at the top of atmosphere for the period 1984–2000

**A. Fotiadi[2], N. Hatzianastassiou[1,2], C. Matsoukas[2,3], K. G. Pavlakis[2],
E. Drakakis[2,4], D. Hatzidimitriou[2,3], and I. Vardavas[2,3]**

[1]Laboratory of Meteorology, Department of Physics, University of Ioannina, Greece
[2]Foundation for Research and Technology-Hellas, Heraklion, Crete, Greece
[3]Department of Physics, University of Crete, Crete, Greece
[4]Department of Electrical Engineering, Technological Educational Institute of Crete, Greece

Correspondence to: N. Hatzianastassiou (nhatzian@cc.uoi.gr)

Title Page

Abstract | Introduction

Conclusions | References

Tables | Figures

◄ | ►►

◄ | ►

Back | Close

Full Screen / Esc

Print Version

Interactive Discussion

EGU

Abstract

A decadal-scale trend in the tropical radiative energy budget has been observed recently by satellites, which however is not reproduced by climate models. In the present study, we have computed the outgoing shortwave radiation (OSR) at the top of atmosphere (TOA) at 2.5° longitude-latitude resolution and on a mean monthly basis for the 17-year period 1984–2000, by using a deterministic solar radiative transfer model and cloud climatological data from the International Satellite Cloud Climatology Project (ISCCP) D2 database. Atmospheric temperature and humidity vertical profiles, as well as other supplementary data, were taken from the National Centers for Environmental Prediction – National Center for Atmospheric Research (NCEP/NCAR) and the European Center for Medium-Range Weather Forecasts (ECMWF) Global Reanalysis Projects, while other global databases, such as the Global Aerosol Data Set (GADS) for aerosol data, were also used. Anomaly time series for the mean monthly pixel-level OSR fluxes, as well as for the key physical parameters, were constructed. A significant decreasing trend in OSR anomalies, starting mainly from the late 1980s, was found in tropical and subtropical regions (30° S–30° N), indicating an increase in solar planetary heating equal to $3.2\pm0.5\,\mathrm{Wm}^{-2}$ over the 17-year time period from 1984 to 2000 or $1.9\pm0.3\,\mathrm{Wm}^{-2}$/decade, reproducing well the features recorded by satellite observations, in contrast to climate model results. The model computed trend is in good agreement with the corresponding linear decrease of $3.7\pm0.5\,\mathrm{Wm}^{-2}$ (or $2.5\pm0.4\,\mathrm{Wm}^{-2}$/decade) in tropical mean OSR anomalies derived from ERBE S-10N non-scanner data. An attempt was made to identify the physical processes responsible for the decreasing trend in tropical mean OSR. A detailed correlation analysis using pixel-level anomalies of OSR flux and ISCCP cloud cover over the entire tropical and subtropical region (30° S–30° N), gave a correlation coefficient of 0.79, indicating that decreasing cloud cover is the main reason for the tropical OSR trend. According to the ISCCP-D2 data derived from the combined visible/infrared (VIS/IR) analysis, the tropical cloud cover has decreased by $6.6\pm0.2\%$ per decade, in relative terms. A de-

EGU

tailed analysis of the inter-annual and long-term variability of the various parameters determining the OSR at TOA, has shown that the most important contribution to the observed OSR trend comes from a decrease in low-level cloud cover over the period 1984–2000, followed by decreases in middle and high-level cloud cover. Opposite but small trends are introduced by increases in cloud scattering optical depth of low and middle clouds.

1. Introduction

The climate of the Earth-atmosphere system is driven by the Earth's radiation budget. Clouds interact with radiation playing thus a key role for the Earth's radiation balance, and hence they strongly affect the Earth's climate. However, cloud-radiation interactions currently introduce the largest uncertainty in climate variability and climatic change prediction through various feedback processes (IPCC, 2001).

In the last few years, there is increasing evidence of a large decadal trend in the top of atmosphere (TOA) tropical radiation budget, attributed to changes in cloud amount (Wielicki et al., 2002a, b; Allan and Slingo, 2002; Chen et al., 2002; Lin et al., 2004; Zhang et al., 2004). This is very important in view of the so-called 'Iris effect' (Lindzen et al., 2001), a very interesting but controversial (Trenberth, 2000) idea of how clouds might act to stabilize our climate system, given the importance of the radiative effects of tropical clouds in the iris feedback (Fu et al., 2002). Wielicki et al. (2002a, b) analysing satellite broadband observations (ERBS WFOV, ERBE/ERBS scanner, ScaRaB, CERES) of the outgoing longwave (OLR) and shortwave radiation (OSR) at TOA over the 22-year period 1979–2001, reported a significant decadal-scale variation of $\sim 3\,\mathrm{Wm^{-2}}$ in the tropical OLR and OSR at TOA. They suggested that this variation is caused by changes in tropical cloudiness as given by the International Satellite Cloud Climatology Project (ISCCP). Chen et al. (2002) using ISCCP data, also reported that there has been a corresponding variation in total cloud amount in tropical and sub-tropical regions, over the same period, that might explain the SW

radiative flux anomalies. They provide evidence that these cloudiness changes are related to changes in vertical air-motion possibly associated with a strengthening of the tropical Hadley and Walker circulations. Jacobowitz et al. (2003) using the Advanced Very High Resolution Radiometer (AVHRR) Pathfinder Atmosphere (PATMOS) climate data set, examined the time series of the OSR at TOA in the tropics (20° S–20° N), and found that tropical PATMOS and ERBS OSR fluxes are in quite good agreement. However, for the OLR at TOA they found no significant long-term trend in the corrected PATMOS data against the significant increasing trend found in ERBE OLR fluxes. Hatzidimitriou et al. (2004) performed an analysis on the tropical OLR at TOA and its causes. They have reported a decadal increase in OLR at TOA of $1.9\pm0.2\,\mathrm{Wm}^{-2}$, mainly attributed to a decrease in high-level cloud cover over the period 1984–2000, followed by a drying of the upper troposphere and a decrease in low-level cloudiness. Zhang et al. (2004) calculated time-series of monthly mean TOA SW and LW fluxes from ISCCP-FD data, confirming that there is a decadal variation in the tropical mean radiative energy budget. It is noteworthy that climate models studied by Wielicki et al. (2002) and Allan and Slingo (2002), failed to reproduce this variation in the tropical energy budget, as measured by satellites, with the currently used climate forcings, due to either some additional external forcing or some internal physical processes which are not included in the climate models (Allan and Slingo, 2002). Most of the existing studies, however, give more emphasis to the decadal trend in OLR rather than OSR flux at TOA, probably because it is generally more difficult to obtain correct SW than LW fluxes in climate models (Wielicki et al., 2002a, data supplement http://www.sciencemag.org/cgi/content/full/295/5556/841/DC1). Besides, in most cases, the existing studies do not examine the causes of the decadal scale trends. Recently Hatzianastassiou et al. (2004a), using a deterministic radiative transfer model along with ISCCP-D2 data, reported a decreasing trend in the OSR flux at TOA, of $2.3\,\mathrm{Wm}^{-2}$ on a global scale, over the 14-year period 1984–1997. This global OSR trend was ascribed to low latitudes, while clouds, as given by ISCCP, were identified as the most likely source. However, there is still some debate on whether the

N. Hatzianastassiou et al.

N. Hatzianastassiou et al.

decreasing trend in cloud amount is physical or not. More detailed investigations are necessary. For example, the impact of various cloud types on the OSR trend, as well as the relationship between the trend in OSR and that in the amount of different cloud types should be determined. Ellis et al. (2004) employing cloud amount data from the ISCCP-D2 and CLAUS dataset (which is, however, based upon ISCCP-D2) provided strong evidence that the cloud amount trend, especially in the tropics, is physical and robust, and that it is significantly correlated with various dynamical parameters.

In this study, we have computed the tropical OSR flux at TOA over the extended 17-year time period from 1984 to 2000 by using a deterministic radiative transfer model, cloud data from ISCCP-D, and atmospheric and humidity data from NCEP/NCAR and ECMWF reanalysis projects. Anomaly time series of the OSR at TOA, as well as of the key input climatological data, averaged over tropical and subtropical regions (30° S–30° N), were constructed to investigate any existing trend. The model OSR anomalies have been compared with those obtained from the Earth Radiation Budget Experiment (ERBE, Barkstrom et al., 1989) ERBS S-10N (WFOV NF edition 2) non-scanner data. Our model results show that, contrary to climate models, the deterministic radiative transfer model can reproduce well the long-term variability in the tropical SW radiation budget at TOA. The sources of this long-term OSR trend were further investigated, and the effect of any long-term changes detected in the time series of the model input data, to changes in the OSR at TOA, was examined.

2. Model and input data

The radiative transfer model used to compute the TOA OSR fluxes, is described in detail by Hatzianastassiou et al. (2004a), Hatzianastassiou and Vardavas (1999, 2001) and Vardavas and Koutoulaki (1995). It was developed from a radiative-convective model (Vardavas and Carver, 1984) and has been successfully tested (cf. Hatzianastassiou and Vardavas, 1999, 2001) according to the Intercomparison of Radiation Codes in Climate Models (ICRCCM) program, as well as against ERBE-S4 scanner

data (cf. Hatzianastassiou et al., 2004a). In brief, the model provides the monthly mean SW radiation budget at TOA on 2.5° longitude-latitude resolution for the 17-year period 1984–2000. The radiative fluxes are computed over two spectral bands: UV-visible ($\lambda < 0.85\,\mu$m) and near-IR ($0.85\,\mu$m$\leq \lambda \leq 5\,\mu$m). The solar radiative transfer in the Earth-atmosphere system is treated separately in each spectral band accounting for absorption and multiple scattering. The model takes into account the presence of ozone (O_3), water vapour (H_2O), carbon dioxide (CO_2), aerosol particles, Rayleigh scattering, surface reflection, and clouds (low, middle, high), while for each pixel the sky is divided into clear and cloudy fractions, and hence direct and diffuse components are considered for solar radiation. Cloud climatological data such as cloud cover and cloud optical thickness are taken from the ISCCP-D2 dataset (Rossow et al., 1996; Rossow and Schiffer, 1999). The ISCCP currently provides the most extensive and comprehensive cloud climatological database that quantifies the variations of cloud properties at global scale for the period starting from 1984 and still continuing. The ISCCP data are based on calibrated narrowband measurements from meteorological satellites whose orbits and calibrations vary during the period of interest (e.g. Klein and Hartmann, 1993; Rossow and Cairns, 1995). However, the most serious calibration changes have been adjusted for in the last ISCCP-D series data (Rossow and Schiffer, 1999). Therefore, the ISCCP is appropriate for studying possible trends, while it is very important that, apart from cloud cover, it also provides cloud optical depth, which is essential for modelling studies. The model required input data for cloud amount and cloud optical depth are taken by the ISCCP-D2, which provides corresponding data for nine cloud types. Subsequently, these data are appropriately grouped into three categories (see Hatzianastassiou and Vardavas, 1999): low-level clouds having top pressures greater than or equal to 680 mb, high-level clouds with top pressures less than 440 mb, and mid-level clouds in between. Low-level clouds are considered to be: Cu, St and Sc clouds. The middle clouds include: Ac, As, and Ns, while Ci, Cs and deep convective clouds are considered as high-level clouds. High clouds are treated as cold ones, while each of the low and middle cloud types is subdivided into liquid- or ice-phase clouds,

Decrease in the tropical mean outgoing shortwave radiation

N. Hatzianastassiou et al.

resulting thus in 15 cloud types. The values for the 15 independent cloud types are appropriately averaged (see Hatzianastassiou and Vardavas, 1999) to obtain data for low-, mid- and high-level clouds required by our model. It should be noted that we have used in this study the ISCCP-D2 individual cloud data derived from the visible/infrared (VIS/IR) analysis rather than the low-, mid- and high-level cloud data, also provided by ISCCP-D2 and derived using the IR-only analysis. This is done because the combined VIS/IR analysis is of better quality than the IR-only one during daytime (Rossow et al., 1996), and thus the VIS/IR cloud products are more appropriate for SW radiation budget studies. Moreover, the VIS/IR (individual) cloud data were found to dramatically improve the SW model results at both TOA and surface, in terms of comparison with ERBE-S4 scanner satellite data, and Baseline Surface Radiation Network (BSRN) and Global Energy Balance Archive (GEBA) site measurements, respectively.

Climatological vertical distributions of temperature and water vapour as well as data of surface pressure, which are used for the model's topography scheme, are taken either from the NCEP/NCAR or the ECMWF Global Reanalysis Projects. Total O_3 column abundance data are taken from the Television Infrared Observational Satellite (TIROS) Operational Vertical Sounder (TOVS) database, whereas aerosol optical properties, i.e. aerosol optical thickness (AOT), single scattering albedo (ω_{aer}) and asymmetry parameter (g_{aer}), are taken from the Global Aerosol Data Set (GADS) (Koepke et al., 1997). The GADS provides only mean monthly climatological values, but at present there is no data base providing such aerosol data for the whole study period 1984–2000 at global scale. There are new satellite-based instruments (e.g. Moderate Resolution Imaging Spectro-Radiometer, MODIS, or Polarization and Directionality of the Earth's Reflectance, POLDER) performing accurate spectral aerosol measurements at global scale, but they have only started their operation from the year 2001. There are some AOT data for the whole period from the Global Aerosol Climatology Project (GACP), but without global coverage, as they only cover the ocean areas. On the other hand, there are AOT data with global coverage from the Total Ozone Mapping Spectrometer (TOMS), but they only extend up to the year 1992. New re-processed AOT data

from TOMS, including also single scattering albedo, ω_{aer} data, will be released soon by the NASA Goddard Space Flight Center (GSFC) and will cover the whole period 1979–2000. In the meantime, as a first step, the model-required aerosol data were derived from GADS in this study. The GADS aerosol data are given at 61 wavelengths extending from 0.25 to 40 μm, 27 of which lie in the SW range, whereas they are given for 8 values of relative humidity (0, 50, 70, 80, 90, 95, 98, and 99%). Given the strong dependence of aerosol optical properties on the ambient relative humidity, the original GADS properties were then re-computed in a realistic way, for actual relative humidity values for the aerosol layer, as explained in detail by Hatzianastassiou et al. (2004b), for each month in the period from January 1984 to December 2000. Subsequently, the computed values of aerosol optical properties were averaged into the UV-visible and near-IR ranges, weighted by the spectral distribution of the incoming solar flux. Though the use of such aerosol climatological data from GADS is probably not the best in terms of inter-annual variability, this affects only slightly the reliability of the results of the present study, since sensitivity tests carried out with our model (Hatzianastassiou et al., 2004a) have shown that aerosols affect the OSR at TOA much less (by one order of magnitude) than clouds.

3. Model validation

The model mean monthly OSR fluxes at TOA were validated against high-quality ERBE-S4 scanner data (on 2.5° longitude-latitude resolution) for the years 1985–1989 (for which ERBE-S4 data are available). The validation was performed at pixel level for all pixels within the 30° S–30° N zone, providing good agreement, with a correlation coefficient R equal to 0.96. The mean difference between model and ERBE fluxes is 1.5 Wm^{-2} with a standard deviation of 8.6 Wm^{-2}. Figure 1 shows the geographical distribution of the 5-year annual average of OSR at TOA as computed with our model and as derived by ERBE-S4 data. There is very good agreement with differences less than 5% over most pixels in the study region. Also, our model reproduces very well the

5-year average annual cycle of OSR over the tropical and subtropical region, as given by ERBE (Fig. 2). Given that the ERBE-S4 scanner data (1985–1989) do not provide long-term time series, the long-term (1985–1999) ERBE S-10N (WFOV NF edition 2) non-scanner data were also used to serve for intercomparison with our model results (see next section). Note that in this case, our model results were downscaled to $5°$ longitude-latitude resolution, to meet the spatial resolution of the ERBE S-10N data.

4. Results and discussion

Hatzianastassiou et al. (2004a) have reported a decreasing trend in the global mean OSR over the 14-year period 1984–1997 claiming that this trend is attributed to low latitudes. In this study, we have extended the study period up to 17 years, i.e. from January 1984 through December 2000, and focus on the zone $30°$ S–$30°$ N where, according to satellite observations, there is a significant trend in OSR. Inter-annual anomalies of the mean monthly OSR fluxes averaged over the zone $30°$ S–$30°$ N, for the period 1984 to 2000, were calculated with the model and are shown in Fig. 3 (solid line). The OSR anomaly shows great variation, up to $\pm 6\,\mathrm{W m^{-2}}$ above or below the 17-year mean. Interesting features can be seen in Fig. 3, such as positive and negative OSR anomalies during El Niño and La Niña events, respectively. A large positive anomaly of $5\,\mathrm{W m^{-2}}$ following the 1986/1987 El Niño event can be seen, as well as the 1989 La Niña. The largest OSR anomaly, exceeding $6\,\mathrm{W m^{-2}}$, is due to the Mount Pinatubo eruption in June 1991 and to the 1991/1992 El Niño event. This increase in the reflected OSR at TOA within the year following the Pinatubo eruption is in good agreement with ERBE S-10N data as shown here, as well as with PATMOS data (Jacobowitz et al., 2003). This rapid increase in OSR is followed by a recovery period. The effects of the strong 1997/1998 El Niño event that were evident in the observed and simulated OLR flux anomalies (Wielicki et al., 2002; Allan and Slingo, 2002; Hatzidimitriou et al., 2004) are not so evident here, although an associated peak exists, consisting in an OSR anomaly that passes from large negative values (about $-6\,\mathrm{W m^{-2}}$) to positive ones ($\sim 1.5\,\mathrm{W m^{-2}}$).

Decrease in the tropical mean outgoing shortwave radiation

N. Hatzianastassiou et al.

EGU

Decrease in the tropical mean outgoing shortwave radiation

N. Hatzianastassiou et al.

However, as will be discussed below, a strong peak related to the 1997/1998 El Niño event appears in the zone 0°–10° S (cf. Fig. 6). Overall, the mean tropical OSR flux is found to have decreased over the period 1984–2000. The cloud cover (A_c) variability, in terms of anomaly time series, over the same period (1984–2000) and the same re-
gion (30° S–30° N) as for OSR, is also given in Fig. 3. The A_c anomalies were derived from the ISCCP-D2 monthly mean data as differences from the 17-year averages. Note that the strong positive anomalies during the summer of 1991 are mostly attributed to low-level clouds and secondarily to mid-level ones. This is due to the fact that after the Mt. Pinatubo eruption, the VIS/IR ISCCP A_c data indicate a notable decrease of thin
cirrus over oceans, accompanied by a comparable increase of altocumulus and cumulus clouds; over land, there are no significant changes (Luo et al., 2002). However, this is a temporary local effect, since the Mt. Pinatubo volcanic aerosol did not have a significant systematic effect on tropical cirrus properties such as cloud amount or optical thickness, as reported by Luo et al. (2002). Linear regressions to the OSR and A_c
anomalies are also given in Fig. 3. The time series of OSR anomaly, exhibit a significant long-term decreasing trend in the tropical and sub-tropical latitudes, well illustrated by the fitted linear regression. More specifically, the model computed OSR anomaly yields a linear decrease equal to $3.2\pm0.5\,\mathrm{Wm^{-2}}$ over the 17-year period from 1984 to 2000 or $1.9\pm0.3\,\mathrm{Wm^{-2}}$/decade. At the beginning of the study period, i.e. around
the mid 1980s, the OSR anomaly is slightly positive, varying around $2\,\mathrm{Wm^{-2}}$, while there is a drop from the late 1980s, down to values of $-2\,\mathrm{Wm^{-2}}$. The positive OSR anomalies at the beginning of the study period are probably due to the influence of the El-Chichon eruption that took place in the spring of 1982. Our model's decreasing trend of $3.2\pm0.5\,\mathrm{Wm^{-2}}$ in tropical and subtropical OSR anomaly is in quite good agreement
with the corresponding value of $\sim3\,\mathrm{Wm^{-2}}$ given by Wielicki et al. (2002a), as derived from satellite records, for the zone 20° S–20° N. Note that the revised value for the OSR flux decrease given by Wielicki et al. (2002b) is $2.5\,\mathrm{Wm^{-2}}$. In terms of comparison with our model results, the corresponding tropical (30° S–30° N) mean OSR anomaly as derived from the ERBE S-10N (WFOV NF edition 2) non-scanner data is overlaid on

N. Hatzianastassiou et al.

EGU

Fig. 3. There is good agreement between the two time series. The linear decrease in tropical OSR anomalies derived by ERBE S-10N data is equal to $3.7\pm0.5\,\mathrm{Wm}^{-2}$ (or $2.5\pm0.4\,\mathrm{Wm}^{-2}$/decade), very close to our model computed value of $3.2\pm0.5\,\mathrm{Wm}^{-2}$ (or $1.9\pm0.3\,\mathrm{Wm}^{-2}$/decade). The slightly larger variability of ERBE anomalies is probably

5 due to the fact that there are missing pixel-level data in the ERBE S-10N in latitudes between 20° and 30° in both hemispheres. Consequently, our deterministic radiative transfer model, unlike climate models, is able to reproduce the decadal-scale trend and the observed patterns of the long-term variability in the OSR at TOA radiative flux anomalies over the tropical regions.

10 It has been suggested (Wielicki et al., 2002a; Chen et al., 2002) that the large decadal variability in tropical OSR is caused by changes in tropical cloudiness. Recently, Hatzianastassiou et al. (2004), based on a sensitivity study, have also reported that the long-term decreasing trend in global mean OSR flux is mostly attributed to cloud cover. In this study, we have performed a thorough analysis identifying clouds as

15 the main source of the model computed decreasing trend in OSR anomalies. At first, this is indicated by the patterns in the tropical mean cloud cover anomalies shown in Fig. 3; these patterns match very well those of OSR flux anomalies. Thus, the tropical cloud cover anomalies depict a decreasing trend, starting from the early 1990s. From 1984 through the late 1980s, the cloud cover has positive anomalies of about 2–4%

20 above the 17-year mean, while after the early 1990s the total A_c anomaly steadily decreases through the late 1990s, reaching values around 4% below the long-term mean value. The overall computed linear decreasing trend in total cloud cover is equal to $6.6\pm0.2\%$ per decade[1]. To further investigate and quantify the apparent correlation between the anomalies of OSR flux and total cloudiness over the tropical region 30° S–

25 30° N, we performed a correlation analysis between the anomalies of model OSR flux and total A_c at $2.5°\times2.5°$ pixel level and on monthly mean basis, for the 17-year period from January 1984 to December 2000; the relevant scatterplot is shown in Fig. 4. The total 704 658 pixel matched data pairs give a correlation coefficient equal to 0.79,

---

[1]Estimated percent decadal trend =100*(parameter decadal change)/(17-year average)

indicating that the decrease in tropical cloud cover is mostly responsible for the satellite-observed and model computed decadal trend (decrease) in tropical OSR at TOA. However, it should be pointed out that, contrary to the ISCCP-D2 A_c data, no trend is found in the adjusted AVHRR PATMOS time series of cloud amount. Besides, no system-
5   atic trends are noticed in the PATMOS tropical OSR and OLR fluxes (Jacobowitz et al., 2003), in contrast to ERBE S-10N. Note also that there is a decreasing trend in the cloud amount time series from the CLAUS dataset, which is consistent with that of ISCCP-D2 A_c data (Ellis et al., 2004). Thus, overall, it is very interesting that in this study, using cloud data derived from the ISCCP-D2 along with surface and atmospheric
10   data from reanalysis projects, we compute a decreasing trend in OSR at TOA, which is in good agreement with the trend found in ERBE S-10N corrected records.

In order to investigate the covariability of the anomalies of OSR at TOA and cloudiness at global scale, the 17-year (1984–2000) time series of monthly mean 10° zonally averaged OSR flux and A_c anomalies were constructed and are plotted in Figs. 5 and
15   6. For each 10° latitude zone, linear regression fits are also plotted for both OSR and A_c anomalies. There is an apparent correlation between the long-term OSR and A_c anomalies, especially in low and middle latitudes. Besides, there are significant decreasing trends in both OSR and A_c anomalies in the latitudes between 50° S and 60° N, especially between 30° S–30° N. We have computed the correlation coefficients
20   of the scatterplot comparison between the pixel-level monthly mean TOA OSR flux anomalies and total A_c anomalies for each 10° latitude zone, over the period 1984–2000. Table 1 summarises the correlation coefficients for each 10° zone between 30° S–30° N, although computations have been also performed for the rest of the globe. Nevertheless, values are not given for latitudes poleward of 30° N and S since, accord-
25   ing to our analysis, the OSR and total A_c anomalies are mostly correlated in the zones between 30° S and 30° N, with correlation coefficients ranging from 0.58 to 0.66. The strongest correlation is found in the tropical latitudes 0°–10° N and S. Indeed, Figs. 5 and 6 confirm that anomalies of OSR flux and total A_c have very similar inter-annual variability patterns between 10° S–10° N, but also between 30° S and 30° N. The corre-

lation coefficient values gradually drop down to 0.17 towards the middle latitudes, and to no significant values in polar areas. Note that, as it has been already mentioned, the El Niño event of 1997/1998 is clearly indicated in the zone 0°–10° S, in both OSR and A_c anomalies. According to Figs. 5 and 6, both cloudiness and OSR flux anomalies

5 have decreasing trends, which are more pronounced in the tropical and subtropical regions, especially in the northern hemisphere. The decreasing trends become smaller towards the middle and high latitudes, where the A_c anomaly becomes even slightly positive. According to our analysis, the low-level clouds show a stronger decreasing trend than mid- and high-level clouds in areas between 30° S–30° N. Furthermore, ac-

10 cording to ISCCP, all three cloud types are found to decrease over the tropical and subtropical areas, apart from high-level clouds that slightly increase in 0°–10° N. In some zones, such as 20° S–30° S and 30° S–40° S, the high-level clouds show a stronger decreasing trend than low- or mid-level ones. In general, the middle and high clouds have increasing trends in the latitudes poleward of 60° N and S, resulting thus in the

15 increasing trend in total cloudiness over polar areas. Nevertheless, despite the slightly increasing trend in total A_c in high latitudes, the corresponding OSR flux anomalies still exhibit decreasing trends. Certainly, such features require further and more detailed investigations. However, note that there is a large number of missing pixel values poleward of 60° N and S, while both multi-year ISCCP-D2 A_c data and hence OSR fluxes,

20 are largely uncertain in polar areas.

We have attempted to determine which of the main climatological parameters (described in Sect. 2) that determine the OSR at TOA, contribute significantly to the observed mean tropical OSR trend (as computed by our model) for the period 1984–2000. The methodology is the following: the anomaly time series of each input parameter

25 were constructed for the period 1984–2000 and for the region 30° S–30° N, in exactly the same way as for the OSR and total cloud cover anomaly time series. Then, the existence of any long-term trend was quantified by applying a simple linear regression analysis, and whenever a statistically significant long-term trend was found for a parameter, this was introduced for the particular parameter in the model. The OSR at

N. Hatzianastassiou et al.

TOA for each year of the study period (1984–2000), and the induced overall change in OSR (in Wm^{-2}) was computed. Table 2 summarises the results of this analysis. All cloud types show a linearly decreasing trend over the study period, with the low-level clouds having the largest trend, equal to $-3.9\pm0.3\%$ in absolute values or $-9.9\pm0.8\%$ per decade in relative terms. Similarly, the mid-level clouds decreased by $1.4\pm0.2\%$ over the period 1984–2000 or by $6.6\pm0.8\%$ per decade, while the high-level ones also decreased by $1.2\pm0.4\%$ or $3\pm0.9\%$ per decade, i.e. less than low and middle clouds. Thus, the VIS/IR mean tropical (30° S–30° N) low-level clouds are found to have undergone the greatest decrease during the period 1984–2000, in agreement with the findings of Chen et al. (2002) and Lin et al. (2004). As for the other parameters, the cloud absorption optical depth for low and middle clouds has increased by $2.8\pm1\%$ and $3.1\pm1.1\%$ per decade, respectively, whereas that of high-level clouds decreased by $5\pm1.4\%$ per decade. The corresponding values for the cloud scattering optical depth are equal to $4\pm0.9\%$, $4.9\pm0.8\%$ and $-0.3\pm1.9\%$ per decade for the low-, mid- and high-level clouds, respectively (the high-level clouds have no significant trend because of large error). Finally, total precipitable water and total ozone column abundance show small decreasing decadal trends.

According to Table 2, the decrease in low-level cloud amount results in a significant decrease in OSR at TOA of $3.1\,Wm^{-2}$, whereas the decreases in mid- and high-level cloud cover have induced smaller decreases in OSR, equal to 1.2 and $1.0\,Wm^{-2}$, respectively. This is normal since (i) the decrease in low-level A_c is larger than that for mid- and high-level A_c (as shown in Table 2), and (ii) the OSR is more sensitive to low clouds rather than to mid- or high-level clouds, as shown by a sensitivity study performed by Hatzianastassiou et al. (2004a). Although the computed decrease in mid-level clouds is greater than that of high-level clouds, the corresponding decrease in OSR induced by the middle clouds is almost equal to the OSR decrease introduced by high-level clouds. This can be explained by the fact that OSR is more sensitive to high-level than to middle clouds (Hatzianastassiou et al., 2004a). Among the other parameters, only the cloud scattering optical depth of low- and mid-level clouds introduces

significant increases in the OSR at TOA, equal to 0.9 and 0.62 Wm^{-2}, respectively. The contribution of the rest of the parameters to the overall OSR trend is minor. Therefore, the observed trend in the tropical mean OSR at TOA (as computed by our model) over the period 1984–2000, is mostly explained by changes in cloud amount, and especially those of low-level clouds, rather than any change in other cloud properties or other physical input parameter. More specifically, the OSR radiative forcing due to low-level clouds represents about 78% of the total OSR forcing induced by all parameters.

5. Conclusions

Our model analysis, using a SW radiative transfer model along with mean monthly climatological data for key physical parameters taken from the ISCCP-D2 data set and the NCEP/NCAR and ECMWF global reanalysis projects, indicates that there has been a decrease in the mean tropical and subtropical (30° S–30° N) OSR at TOA of 3.2±0.5 Wm^{-2} over the 17-year period from January 1984 to December 2000 (or 1.9±0.3 Wm^{-2}/decade). This decrease is in good agreement with the results of Wielicki et al. (2002a, b) and close to the computed value of 3.7±0.5 Wm^{-2} derived from the long-term ERBE S-10N (WFOV NF edition 2) non-scanner OSR time series. The 17-year (1984–2000) time series of anomalies in both OSR flux at TOA and various physical parameters were constructed as departures from the corresponding 17-year mean values. The performed correlation analysis between mean monthly pixel-level anomalies of model OSR flux at TOA and VIS/IR ISCCP-D2 total cloud cover over the tropical and subtropical regions (30° S–30° N), has shown a significant correlation, with a coefficient equal to 0.79 at the 95% significance level. Our analysis of the inter-annual and long-term variability of the various parameters determining the OSR at TOA, has shown that the most important contribution to the observed OSR trend comes from a decrease in VIS/IR low-level cloud amount over the period 1984–2000, followed by smaller decreasing trends in mid- and high-level cloudiness. Opposite but small trends are introduced by an increase in cloud scattering optical depth of low clouds,

and a smaller increase for middle-level clouds. Finally we note that the OSR trend of 1.9±0.3 Wm^{-2}/decade as computed by our model, is balanced by the OLR trend of 1.9±0.2 Wm^{-2}/decade computed by Hatzidimitriou et al. (2004) using a corresponding deterministic LW radiative transfer model, resulting thus in an absence of any decadal trend in the net (all-wave) radiation budget at TOA during our study period.

References

Allan, R. P. and Slingo, A.: Can current climate forcings explain the spatial and temporal signatures of decadal OLR variations?, Geophys. Res. Lett., 29(7), 1141, doi:10.1029/2001GL014620, 2002.

Barkstrom, B., Harrison, E., Smith, G., Green, R., Kibler, J., Cess, R., and ERBE Science team: Earth Radiation Budget Experiment (ERBE) archival and April 1985 results, Bull. Am. Meteorol. Soc., 70, 1254–1262, 1989.

Chen, J., Carlson, B. E., and Del Genio, A. D.: Evidence for strengthening of the tropical general circulation in the 1990s, Science, 295, 838–841, 2002.

Ellis, T. D., Stephens, G. L., and Thompson, D. W.: Evaluation of cloud amount trend and connections large scale dynamics, 15th Symposium on Global Change and Climate Variations, The 84th AMS Annual Meeting, 11–15 January 2004, Seattle, WA, USA, (http://reef.atmos.colostate.edu/ellis/AMStalk.html).

[Title Page](#)

[Abstract](#) [Introduction](#)

[Conclusions](#) [References](#)

[Tables](#) [Figures](#)

[◄](#) [►](#)

[◄](#) [►](#)

[Back](#) [Close](#)

[Full Screen / Esc](#)

[Print Version](#)

[Interactive Discussion](#)

[EGU](#)

Fu, Q., Baker, M., and Hartmann, D. L.: Tropical cirrus and water vapour feedback: an effective earth infrared iris feedback?, Atmos. Chem. Phys., 2, 31–37, 2002, SRef-ID: 1680-7324/acp/2002-2-31.

Hatzianastassiou, N. and Vardavas, I.: Shortwave radiation budget of the Northern Hemisphere
5   using International Satellite Cloud Climatology Project and NCEP/NCAR climatological data, J. Geophys. Res., 104, 24 401–24 421, 1999.

Hatzianastassiou, N. and Vardavas, I.: Shortwave radiation budget of the Southern Hemisphere using ISCCP C2 and NCEP/NCAR climatological data, J. Climate, 14, 4319–4329, 2001.

Hatzianastassiou, N., Fotiadi, A., Matsoukas, C., Drakakis, E., Pavlakis, K. G., Hatzidimitriou,
10   D., and Vardavas, I.: Long-term Global Distribution of Shortwave Radiation Budget at the Top of Atmosphere, Atmos. Chem. Phys., 4, 1217–1235, 2004a, SRef-ID: 1680-7324/acp/2004-4-1217.

Hatzianastassiou, N., Katsoulis, B., and Vardavas, I.: Global distribution of aerosol direct radiative forcing in the ultraviolet and visible arising under clear skies, Tellus, 56B, 51–71, 2004b.

15   Hatzidimitriou, D., Vardavas, I., Pavlakis, K. G., Hatzianastassiou, N., Matsoukas, C., and Drakakis, E.: On the decadal increase in the tropical mean outgoing longwave radiation for the period 1984–2000, Atmos. Chem. Phys., 4, 1419–1425, 2004, SRef-ID: 1680-7324/acp/2004-4-1419.

Intergovernmental Panel on Climate Change (IPCC): Climate Chance 2001: The Scientific
20   Basis, edited by: Houghton, J., Ding, Y., Griggs, D. J., Noguer, M., Van der Linden, P. J., Dai, X., Maskell, K., and Johnson, C. A., Cambridge University Press, Cambridge, 881, 2001.

Jacobowitz, H., Stowe, L. L., Ohring, G., Heidinger, A., Knapp, K., and Nalli, N. R.: The Advanced Very High Resolution Radiometer Pathfinder Atmosphere (PATMOS) Climate Dataset: A resource for Climate Research, Bull. Am. Meteor. Soc., 84, 785–793, 2003.

25   Klein, S. A. and Hartmann, D. L.: Spurious changes in the ISCCP data set, Geophys. Res. Lett., 20, 455–458, 1993.

Koepke, P., Hess, M., Schult, I., and Shettle, E. P.: Global aerosol data set, Rep. No 243, Max-Plank Institute fur Meteorologie, Hamburg Germany, 44, 1997.

Lindzen, R., Chou, M.-D., and Hou, A.: Does the earth have an adaptive infrared iris?, Bull.
30   Am. Meteorol. Soc., 82, 417–432, 2001.

Lin, B., Wong, T., Wielicki, B. A., and Hu, Y.: Examination of the Decadal Tropical Mean ERBS Nonscanner Radiation Data for the Iris Hypothesis, J. Climate, 17, 1239–1246, 2004.

Luo, Z., Rossow, W. B., Inoue, T., and Stubenrauch, C. J.: Did the eruption of the Mt. Pinatubo

Decrease in the tropical mean outgoing shortwave radiation

N. Hatzianastassiou et al.

EGU

volcano affect cirrus properties?, J. Climate, 15, 2806–2820, 2002.

Rossow, W. B. and Cairns, B.: Monitoring changes of clouds, Climate Change, 31, 305–347, 1995.

Rossow, W. B. and Schiffer, R. A.: Advances in understanding clouds from ISCCP, Bull. Am. Meteorol. Soc., 80, 2261–2287, 1999.

Rossow, W. B., Walker, A. W., Beuschel, D. E., and Roiter, M. D.: International Satellite Cloud Climatology Project (ISCCP). Documentation of new cloud datasets, World Meteorol. Org., Geneva, 115, 1996.

Trenberth, K. E.: Changes in Tropical Clouds and Radiation, Science, 296, 2095, 2002.

Vardavas, I. and Carver, J. H.: Solar and terrestrial parameterizations for radiative convective models, Planet. Space Sci., 32, 1307–1325, 1984.

Vardavas, I. M. and Koutoulaki, K.: A model for the solar radiation budget of the Norther Hemisphere: Comparison with Earth Radiation Budget Experiment data, J. Geophys. Res., 100, 7303–7314, 1995.

Wielicki, B. A., Wong, T. M., Allan, R. P., Slingo, A., Kiehl, J. T., Soden, B. J., Gordon, C. T., Miller, A. J., Yang, S.-K., Randall, D. A., Robertson, F., Susskind, J., and Jacobowitz, H.: Evidence for large decadal variability in the tropical mean radiative energy budget, Science, 295, 841–844, 2002a.

Wielicki, B. A., Del Genio, A. D., Wong, T., Chen, J., Carlson, B. A., Allan, R. P., Robertson, F., Jacobowitz, H., Slingo, A., Randall, D. A., Kiehl, J. T., Soden, B. J., Gordon, C. T., Miller, A. J., Yang, S., and Susskind, J.: Changes in Tropical Clouds and Radiation, Response, Science, 296, 2095a, 2002b.

Zhang, Y., Rossow, W. B., Lacis, A. A., Oinas, V., and Mishchenko, M. I.: Calculation of radiative fluxes from the surface to top of atmosphere based on ISCCP and other global data sets: Refinements of the radiative transfer model and the input data, J. Geophys. Res., 109, D19105, doi:10.1029/2003JD004457, 2004.

Decrease in the tropical mean outgoing shortwave radiation

N. Hatzianastassiou et al.

Title Page

Abstract | Introduction

Conclusions | References

Tables | Figures

◄ | ►

◄ | ►

Back | Close
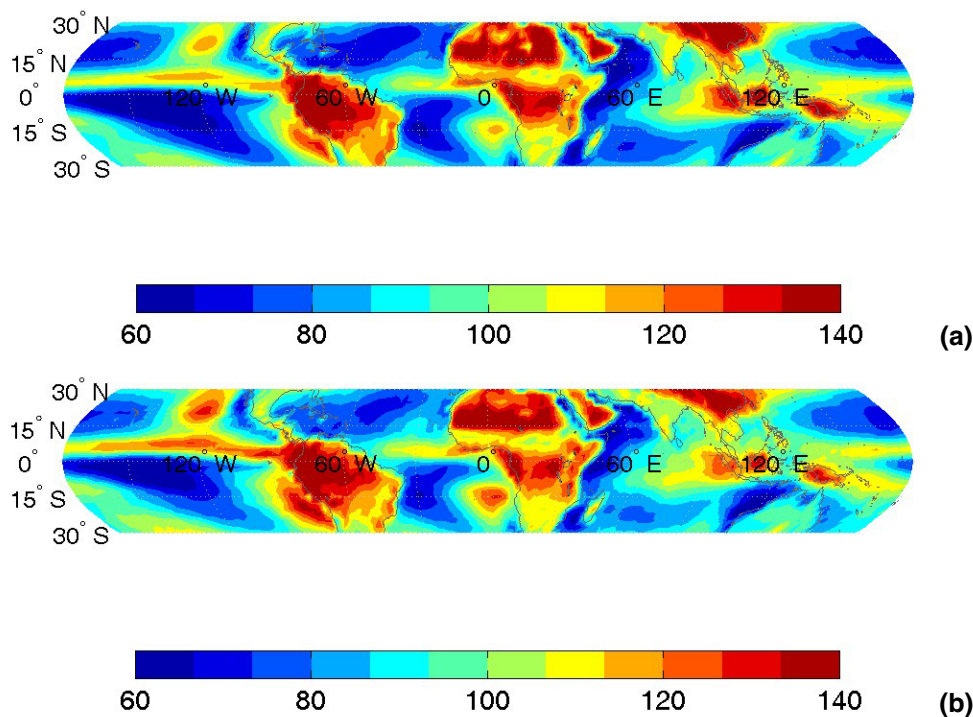
Full Screen / Esc

Print Version

Interactive Discussion

EGU

EGU

Table 1. Correlation coefficient (R^2) values of the scatter plot comparison between the pixel-level monthly mean top of atmosphere (TOA) outgoing shortwave radiation (OSR) anomalies and total cloud cover (A_c) anomalies for each 10° latitude zone between 30° S–30° N, over the time period 1984–2000.

Zones (°)	R^2 (OSR – total A_c)
20°–30° N	0.58
10°–20° N	0.59
0°–10° N	0.65
10°–0° S	0.66
20°–10° S	0.61
30°–20° S	0.62

Decrease in the tropical mean outgoing shortwave radiation

N. Hatzianastassiou et al.

Table 2. Decadal linear trend in low-, mid- and high-level cloud cover (A_c), cloud absorption optical depth (τ_c^a), cloud scattering optical depth (τ_c^s), total precipitable water (W_{H2O}), and total ozone column abundance (W_{O3}) for the 30^oS-30^oN region, and the corresponding induced changes (radiative forcing in Wm^{-2}) in the outgoing shortwave radiation (OSR) at the top of atmosphere (TOA).

Parameter	Decadal Trend (%)	OSR radiative forcing at TOA (Wm^{-2})
A_c – Low	−9.9±0.8	3.1↓
A_c – Middle	−6.6±0.8	1.2↓
A_c – High	−3.0±0.9	1.0↓
Low – τ_c^a	2.8±1.0	0.16↓
Middle – τ_c^a	3.1±1.1	0.11↓
High – τ_c^a	−5.0±1.4	0.02↑
Low – τ_c^s	4.0±0.9	0.9↑
Middle – τ_c^s	4.9±0.8	0.62↑
High – τ_c^s	−0.3±1.9	0.08↓
W_{H2O}	−1.2±0.3	0.04↑
W_{O3}	−1.3±0.2	0.11↑

Print Version

Interactive Discussion

EGU

Fig. 1. Geographical distribution of the outgoing shortwave radiation (OSR) at the top of atmosphere (TOA), **(a)** as calculated by the model and **(b)** as derived by ERBE-S4 scanner data. Both give the annual long-term average calculated over the 60-month period covered by the ERBE-S4 dataset (1985–1989).
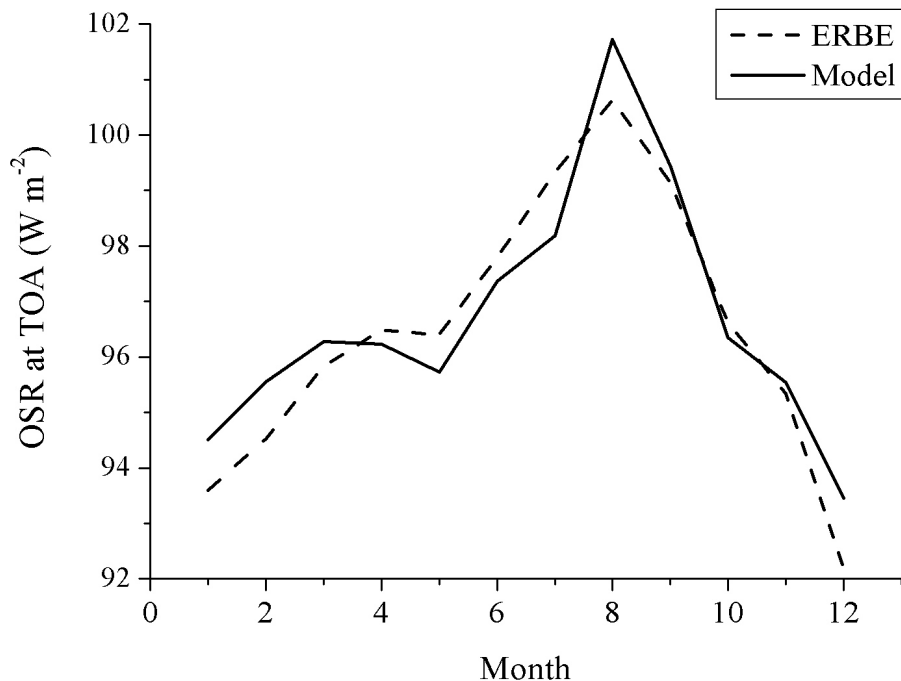
EGU

Fig. 2. Average seasonal cycle displayed by the model OSR (solid line) and the ERBE OSR (dashed line), after having subtracted from the model data the value of $1.5\,\text{Wm}^{-2}$ (model bias).
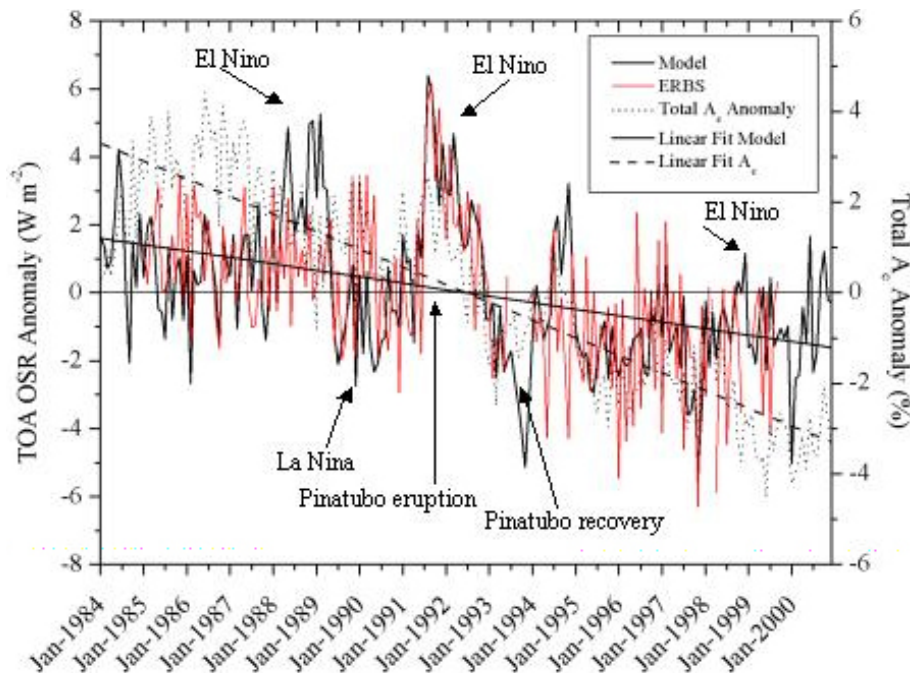
Fig. 3. Time series of tropical (30° S–30° N) mean model (black solid line) and ERBE S-10N (red solid line) top of atmosphere (TOA) outgoing shortwave radiation (OSR) anomalies (in Wm^{-2}), and ISCCP-D2 total cloud cover (A_c) anomalies (in %) (dotted line), over the time period 1984–2000. Linear regression fits to the model OSR flux anomaly (bold solid line) and A_c anomaly (dashed line) are also shown.
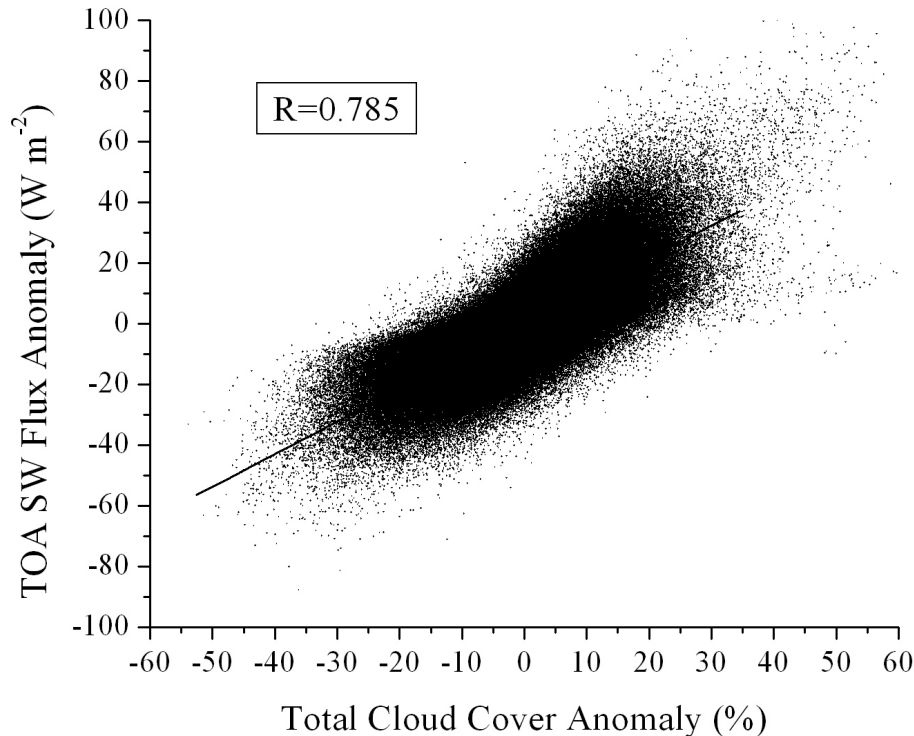
Fig. 4. Scatterplot comparison between the pixel-level monthly mean top of atmosphere (TOA) outgoing shortwave flux anomalies (in Wm^{-2}) and the ISCCP-D2 total cloud cover anomalies (%) for the region 30° S–30° N, over the period 1984–2000. A total number of 704 658 box matched data pairs are plotted, and the fitted linear regression and correlation coefficient (R) are also given.

Decrease in the tropical mean outgoing shortwave radiation
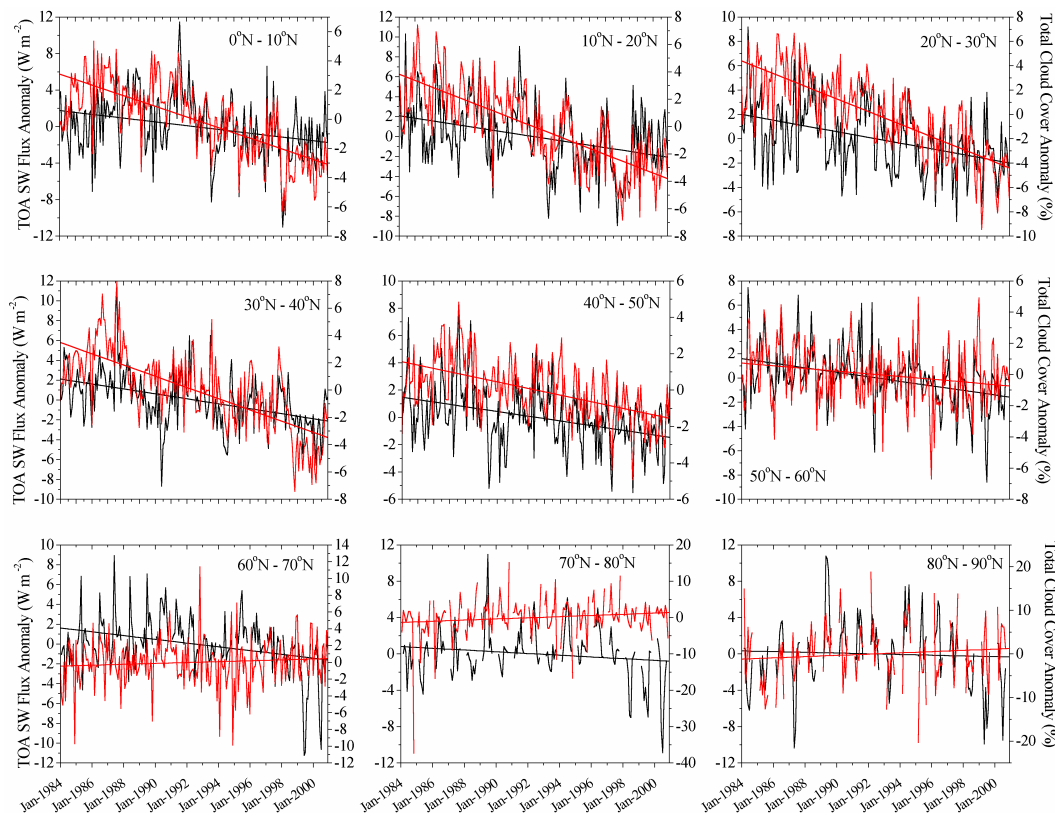
N. Hatzianastassiou et al.

Fig. 5. Time series of 10° latitude zonal averages of the anomalies of top of atmosphere (TOA) outgoing shortwave radiation (OSR) flux (in Wm^{-2}, black lines) and total cloud cover (%, red lines) for the North Hemisphere, over the period 1984–2000. Linear regression fits to the OSR and A$_c$ anomalies are also displayed.
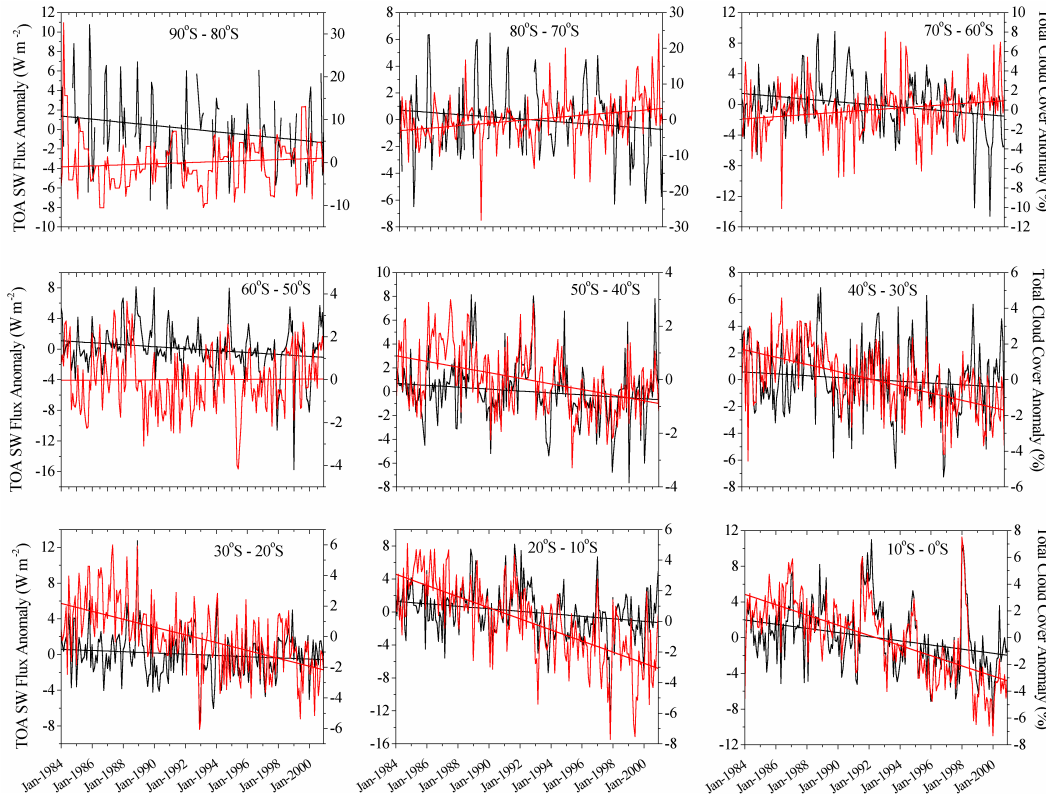
Fig. 6. As in Fig. 5, but for the South Hemisphere.

Title Page

Abstract | Introduction

Conclusions | References

Tables | Figures

◄ | ►►

◄ | ►

Back | Close

Full Screen / Esc

Print Version

Interactive Discussion